SDEMPED 2005 - International Symposium on
Diagnostics for Electric Machines, Power Electronics and Drives
Vienna, Austria, 7-9 September 2005

Wigner-Ville Distributions for Detection of Rotor Faults in Brushless DC (BLDC) Motors Operating Under Non-Stationary Conditions

S. Rajagopalan[1], J. A. Restrepo[2], J. M. Aller[2], T. G. Habetler[1], R. G. Harley[1]

[1]School of Electrical and Computer Engineering
Georgia Institute of Technology
Atlanta GA 30332-0250 USA
thabetler@ece.gatech.edu

[2]Universidad Simón Bolívar
Caracas 1080A, VENEZUELA
restrepo@usb.ve

***Abstract*— Electric motors often operate under operating conditions that are constantly changing with time. Most of such applications demand high reliability from the motor. Early detection of developing motor faults could help provide this needed reliability. While diagnostics of faults in motors operating under steady state conditions is straight forward due to the use of the well known Fourier transformation, diagnostics of motors operating under non-stationary conditions may need more sophisticated signal processing. In this paper, the Wigner-Ville family of time-frequency distributions is presented as an alternative to short time Fourier transforms (STFTs) and wavelets, for the diagnostics of rotor faults in a BLDC motor. Wigner-Ville distributions possess better frequency resolution than the STFT and wavelets. Several variants of the Wigner-Ville distributions are presented. The drawbacks of these distributions and methods to overcome them are also presented. Simulation and experimental results demonstrate that the Wigner-Ville distributions can be a viable tool to analyze rotor faults in BLDC motors operating under continuous non-stationarity.**

Keywords- Wigner-Ville; Pseudo Wigner-Ville; Diagnostics, Rotor faults; BLDC motors; Non-stationary operation

I. INTRODUCTION

In many motor applications, the operating conditions (speed and load) continuously change with time. Such applications are commonly encountered in the aerospace and transportation industries where high motor reliability is a critical factor in maintaining and improving process uptimes as well as providing increased safety to humans. Redundancy and conservative design techniques have been widely adopted for improving the reliability of motors [1]. As an alternative to these expensive techniques, diagnostic strategies and control schemes can be devised to ensure a fault-tolerant control drive. Early detection of potential motor faults and asymmetries through electronic condition monitoring of these machines could therefore provide enhanced reliability and added value. Detection of faults in motors operating under steady state conditions has been widely investigated and the well known Fourier transformation has been the most commonly used tool [2-3]. However, the Fourier transformation is not the best tool to be applied in the analysis of non-stationary signals. This important limitation of the Fourier transformation raises the need for more sophisticated signal processing techniques for the analysis of non-stationary signals. The stator current of a BLDC motor operating in a non-stationary condition is shown in Fig. 1. In such non-stationary applications, both the frequency and amplitude of the motor current are continuously changing with time.

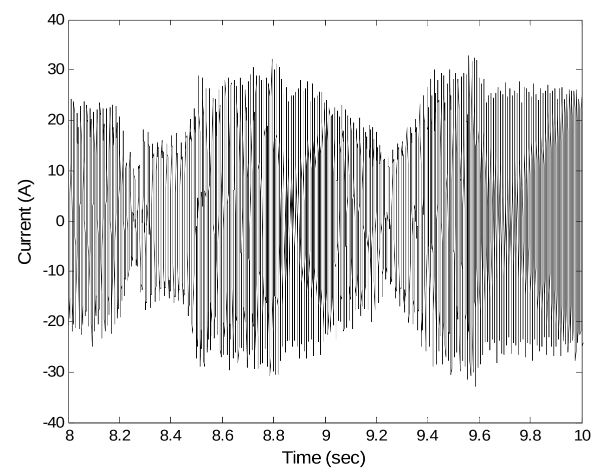

Figure 1. Non-stationary stator current in a BLDC motor.

There has not been much research in the area of fault diagnostics of motors operating under non-stationary conditions and what has been reported is limited to induction motor applications. In [4] the authors use the short-time Fourier transform (STFT) and pattern recognition techniques to detect faults in induction motors operating in varying operating conditions. The STFT is a simple and robust tool. However, it still assumes that the non-stationary signal is slowly changing in a chosen time window. This and the choice of window length impair the use of STFT at low frequencies or when the signal is changing very fast dynamically. This limits the use of STFTs to applications such as rolling steel mills, where the operating conditions change slowly and there are sufficient intervals of time where the motor can be assumed to operate in a stationary condition. The use of discrete wavelets has also been reported for a similar problem [5]. However, the problems of translation variance and the inability of discrete wavelets to closely approximate sinusoidal signals make their use difficult in rotor fault diagnostics. Non-stationary signal analysis has been also been used in the detection of machine faults from the starting current transients in induction motors [6]. This enables the detection of faults under no load condition where the only measurable and useful current exists during the starting of the motor. However, no research has been reported in the diagnosis of motor faults in applications where the motor is operating continuously in a non-stationary state or where assumptions of local or slow stationarity may be questionable and unrealistic.

In this paper, the Wigner-Ville family of time-frequency distributions is presented as a novel alternative to STFT and wavelets, for the diagnostics of rotor faults in a BLDC motor. Several variants of the Wigner-Ville distributions are explained in this paper. The drawbacks of these distributions and methods to overcome them are also presented. Simulation and experimental results are presented to demonstrate that the Smoothed Pseudo Wigner-Ville distribution is a viable tool to analyze faults in motors operating under continuous non-stationarity.

II. Rotor Fault Detection in BLDC Motors Operating Under Non-Stationary Conditions

Potential faults in BLDC machines can be categorized as stator faults, rotor faults, bearing faults, and inverter faults. Rotor faults could be due to eccentricities, unbalanced rotors, damaged rotor magnets, misalignments, and asymmetries [7]. Rotor eccentricities occur when there is a non-uniform air-gap between the stator and the rotor and are classified into two main types: static and dynamic, with the latter being the more severe of the two [8]. If the eccentricity were to become large, the resulting unbalanced radial forces could cause the stator and rotor to rub, resulting in damage to both the stator and the rotor. In the case of the static air-gap eccentricity, the position of the minimal radial air-gap length is fixed in space. In the case of dynamic eccentricity, the center of the rotor is not at the center of rotation, and the position of the minimum air-gap rotates with the rotor. Mechanically unbalanced rotors are usually caused by misaligned load. This unbalance causes slight dynamic eccentricity and motor vibration, eventually leading to motor bearing failure. Detecting dynamic eccentricity and mechanically unbalanced rotors is the focus of this paper.

It is known that rotor defects such as a dynamic eccentricity can be detected by monitoring certain characteristic fault frequencies in the stator current of BLDC motors operating at constant speed [7]. These frequencies are given by

$$f_{rf} = f_e \pm k \frac{f_e}{P/2}, \tag{1}$$

where f_{rf} is the rotor fault frequency, f_e is the fundamental frequency, P is the number of poles in the BLDC machine, and k is any integer. These fault frequencies are also present when the current is non-stationary and will be tracked using the proposed WVD based detection algorithm.

III. Wigner-Ville Distributions (WVD)

Time-frequency analysis consists of the three-dimensional time, frequency, and amplitude representation of a signal, which is inherently suited to indicate transient events in a signal. The Wigner distribution and its various permutations is an analysis technique which has been widely used in the diagnostics of faults in mechanical systems, the most common being the gear train. The Wigner-Ville distribution (WVD) is derived by generalizing the relationship between the power spectrum and the autocorrelation function for non-stationary time-variant processes. The Wigner-Ville distribution of a signal *s(t)* is given by [9-11]

$$W(t,\omega) = \frac{1}{2\pi} \int e^{-j\omega\tau} s^*\left(t - \frac{\tau}{2}\right) s\left(t + \frac{\tau}{2}\right) d\tau , \tag{2}$$

where t is time and ω is frequency. The WVD is a part of a more general distribution called the Cohen class of generalized t-f distributions [9], $\rho(t,f)$, given by

$$\rho(t,\omega) = \frac{1}{4\pi^2} \iiint e^{j\theta(u-t)} \phi(\theta,\tau) s^*\left(u - \frac{\tau}{2}\right) s\left(u + \frac{\tau}{2}\right) e^{-j\omega\tau} d\theta du d\tau , \tag{3}$$

where $\varphi(\theta,\tau)$ is an arbitrary function called the kernel. Setting the kernel $\varphi(\theta,\tau) = 1$ yields the well known Wigner-Ville distribution. It is a high resolution technique offering much better frequency resolution than the STFT. Moreover, the distribution can be used for the analysis of true non-stationary signals without any underlying assumptions.

IV. Variants of Wigner-Ville Distributions (WVD)

The WVD being a bi-quadratic distribution produces large undesirable frequency components called cross-terms that can hamper the interpretation of the distribution. Ghosts and artifacts are also produced; however they are usually smaller in magnitude and can be removed by thresholding. These cross-terms are significantly larger in amplitude when compared to the actual spectral components (also called as auto-terms) in the signal. There are several variants of the WVD that attempt to suppress such cross-terms and the two prominent ones are:

i. Pseudo-Wigner Ville distribution (PWVD).

ii. Smoothed Pseudo Wigner Ville distribution (SPWVD).

The PWVD is the windowed version of the Wigner Ville distribution. The PWVD may be defined in the time domain or in the frequency domain, though the former is more common. Also called the Windowed-Wigner distribution, the PWVD suppresses cross-terms present in the original Wigner distribution and has much better resolution than the STFT [12]. The PWVD is defined in (4), where $h(\tau)$ is the time smoothing window.

$$W_P(t,\omega) = \frac{1}{2\pi}\int e^{-j\omega\tau} h(\tau) s^*\left(t-\frac{\tau}{2}\right) s\left(t+\frac{\tau}{2}\right) d\tau \, . \tag{4}$$

The smoothed WVD (SPWVD) uses a function that smoothes the distribution in both the time and frequency planes. The SPWVD offers better cross-term suppression though at the cost of frequency resolution. This smoothing function is usually Gaussian though windows such as Hamming can be used. The SPWVD is given by [9]

$$W_S(t,\omega) = \int L(t-t', \omega-\omega') W(t',\omega') \, dt' d\omega' \, , \tag{5}$$

where L is the chosen smoothing window (usually Gaussian) applied to the Wigner-Ville distribution $W(t,\omega)$. The commonly used Gaussian window is given by

$$L(t,\omega) = \frac{1}{\alpha\beta} e^{-\frac{t^2}{\alpha} - \frac{\omega^2}{\beta}}, \quad \alpha\beta \geq 1. \tag{6}$$

V. Comparison of WVD Variants

The viability of using the WVDs is first verified through simulation. However, two significant problems arise when applying the WVD or its variants to diagnose rotor faults in BLDC motors:

a. Interaction between the fundamental frequency and the fault frequencies in (5) produce cross-terms at the same values as some fault frequencies produced by (1). These cross-terms may be difficult to suppress even using the PWVD or the SPWVD as the fundamental frequency is several orders in magnitude bigger than the fault components.

b. If a real signal is used as is the stator current of a BLDC motor, then there is both a positive and a negative frequency part to the WVD spectrum which will produce cross terms between it and the positive frequencies. These cross-terms can be eliminated by eliminating the negative frequency terms.

The problem in (a) can be solved by adaptively filtering the fundamental and other inverter harmonics. For motors with large number of poles, certain harmonics may be selectively filtered using an adaptive comb filter prior to signal processing such that cross-terms at desired fault frequencies may be avoided. The PWVD or SPWVD can then be used to suppress any remaining cross-term that may be produced due to interaction with the fundamental.

The negative frequency terms (b) and other artifacts can be removed by converting the real signal to an analytic version of the same using the Hilbert transform. The use of the analytic signal also eliminates the need to sample at twice the Nyquist rate [12]. The analytic signal of a real-valued signal s(t) can be defined as

$$s_A(t) = s(t) + js_H(t) \, , \tag{7}$$

where $s_H(t)$ is the Hilbert transform of the signal $s(t)$ and is given by

$$H[s(t)] = s_H(t) = \frac{1}{\pi}\int_{-\infty}^{\infty} s(\tau)\frac{1}{t-\tau} d\tau \, . \tag{8}$$

The Fourier transform $S_A(f)$ of the analytic signal in (7) does not possess negative frequency components as can be seen from (9) where $S(f)$ is the Fourier transform of $s(t)$ and $S_H(f)$ is the Fourier transform of $s_H(t)$.

$$\begin{aligned} S_A(f) &= S(f) + jS_H(f) = S(f) + \operatorname{sgn} f \; S(f) \\ &= \begin{cases} 0, & if \;\; f\langle 0 \\ S(f), & if \;\; f = 0 \\ 2S(f), & if \;\; f\rangle 0 \end{cases} . \end{aligned} \tag{9}$$

A hypothetical test signal, i_a, approximating a rotor fault scenario and having a fundamental of amplitude 0.04 A (corresponding to a filtered stator current) with two rotor fault sidebands of amplitude 0.05 A is generated using

$$\begin{aligned} i_a &= 0.04\cos\left(2\pi p(t)t\right) + 0.05\cos\left(4\pi p(t)t/3\right) \\ &\quad + 0.05\cos\left(8\pi p(t)t/3\right). \end{aligned} \tag{10}$$

The three frequencies in (10) are the fundamental frequency $p(t)$ and two rotor fault frequencies at 2/3rd and 4/3rd of the fundamental frequency $p(t)$. The amplitudes in (10) were chosen arbitrarily to imitate a rotor fault scenario as close as possible. The frequency $p(t)$ is varied sinusoidally between 0 to 120 Hz. The Rice University Time Frequency Analysis toolbox [13] for MATLAB is used to compute the Wigner distributions for the simulated motor current signal. Fig. 2 is a two dimensional time-frequency (t-f) plot that shows the STFT of the signal i_a. A Hamming window of length 0.25 seconds is used in computing the STFT. The length was chosen through trial and error to obtain the best possible time-frequency resolution. Fig. 3 is a t-f plot that shows the WVD of the signal obtained using (2). The PWVD and the SPWVD of the signal obtained using (4) and (5) respectively, are shown in the t-f plots of Figs. 4 and 5. The t-f plots shows the variation of the multiple frequency components of the signal i_a over time. A Hamming window of length 0.25 seconds is again used for both the PWVD and the SPWVD to facilitate a fair comparison with the STFT. The WVD, PWVD, and the SPWVD are calculated for the analytic version of the real-valued motor current signal. The analytic signal is obtained from the real-valued ia in (10) using (7) and (8).

It can be seen from Figs. 2 and 3 that the WVD provides better frequency resolution than the STFT at lower frequencies, but suffers from a large number of ghosts and artifacts. The PWVD of the Hilbert transformed signal (Fig. 4) shows that much of the interference is removed, thus offering excellent tracking of the fault signals. Some cross-terms are still present. However, the SPWVD in Fig. 5 offers complete suppression of cross-terms while still offering better frequency resolution than

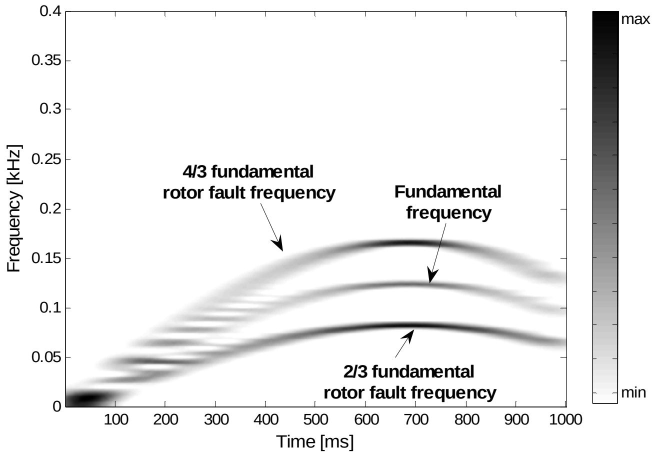

Figure 2. STFT of a simulated BLDCM rotor fault using a hypothetical test signal i_a.

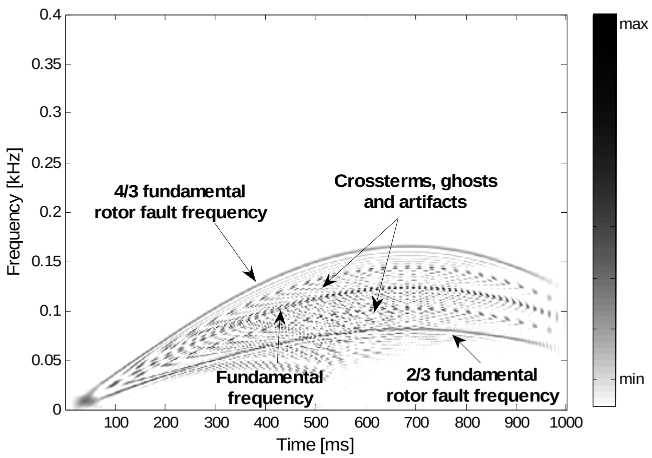

Figure 3. WVD of a simulated BLDCM rotor fault using a hypothetical test signal i_a.

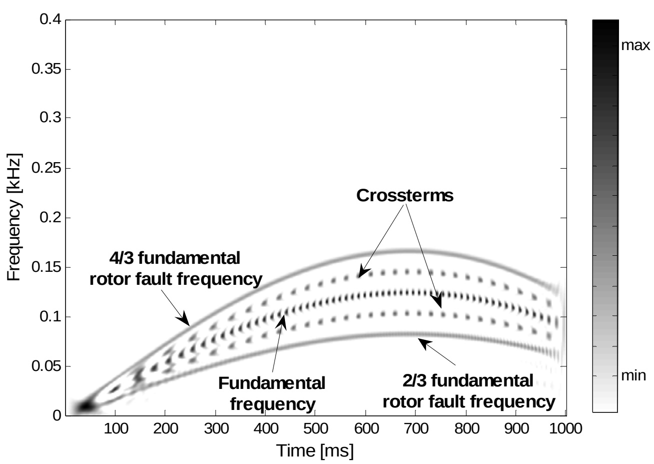

Figure 4. PWVD of a simulated BLDCM rotor fault using a hypothetical test signal i_a .

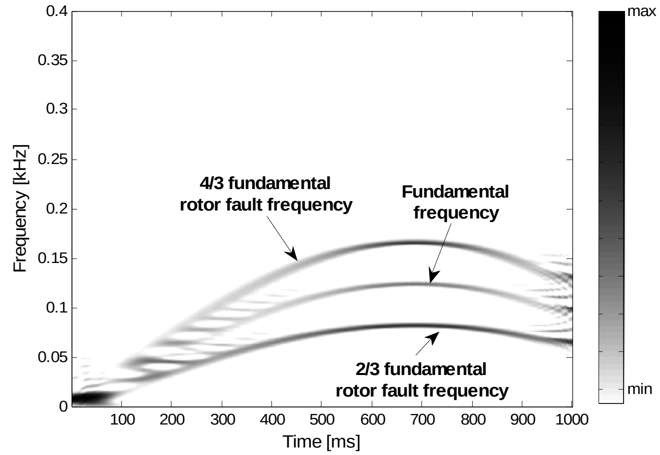

Figure 5. SPWVD of a simulated BLDCM rotor fault using a hypothetical test signal i_a .

the STFT of Fig. 2. Fig. 2 also shows that the spectral components produced by the STFT are smeared in the frequency domain. Hence the fault frequencies are not localized but spread over a frequency range. The PWVD and the SPWVD t-f plots in Figs. 4 and 5 show a much better concentration of energy in the frequency domain. This allows the PWVD and the SPWVD to provide more accurate indication of the fault harmonic amplitudes when compared to the STFT.

VI. PROPOSED SPWVD/PWVD BASED FAULT DETECTION ALGORITHM

The acquired BLDC stator current is first filtered adaptively to remove the fundamental frequency and other inverter harmonics. The filtered stator current is then converted into an analytic signal using the Hilbert transformation explained in the previous section. The SPWVD or the PWVD is then calculated for a time slice of predetermined length. The length is usually a power of 2 to facilitate fast computation. The fault frequencies obtained from the SPWVD / PWVD calculation are then used to compute a fault metric that indicates the health of the motor. A simple RMS fault based metric is used in this research and is given by (11),

$$RMS\ Fault\ Metric = \sqrt{\frac{1}{N}\sum_{i=1}^{i=N} f_i\left(t\right)}, \qquad (11)$$

where $f_i(t)$ is the amplitude of the instantaneous rotor fault frequencies extracted using either the PWVD or the SPWVD algorithms (Fig. 5) and N is the number of fault frequencies extracted at any point in time. A threshold that varies with the amplitude of the fundamental can then be used by the RMS fault metric of (11) to classify the severity of the rotor fault. The complete proposed algorithm is depicted in Fig. 6.

VII. EXPERIMENTAL RESULTS

A BLDC motor controller with 6 poles and rated for 1 kW at 12V is used in the experiments (Fig. 7). The motor controller

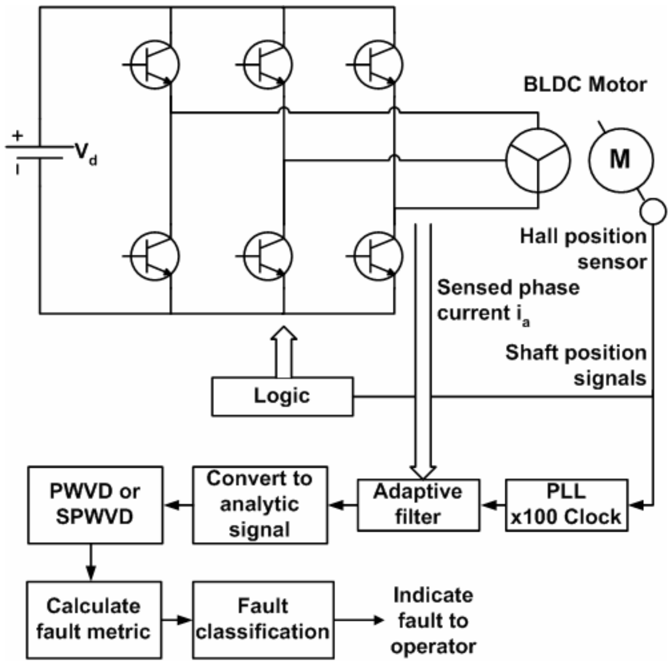

Figure 6. SPWVD / PWVD based BLDC rotor fault detection.

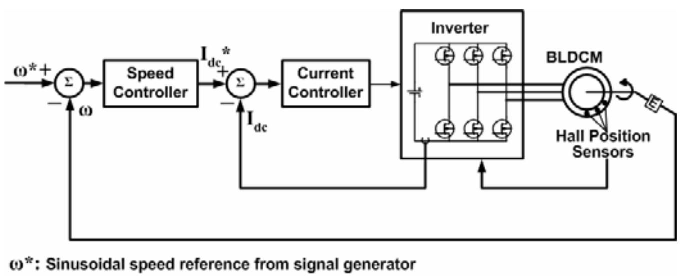

Figure 7. Block diagram of BLDC motor controller.

is provided with both a speed controller and a current controller. One of the phase currents is sensed using Hall current sensors. Adaptive filtering of selected frequencies is done to avoid cross-term generation at rotor fault frequencies. In this experiment, an order 6 analog switched capacitor elliptic filter is used to filter the fundamental and all frequencies above the second harmonic. Clocking for the filter is obtained from the BLDC motor's Hall position sensors using a Phase Locked Loop (PLL). The experimental arrangement is shown in Fig. 8. The filtered stator currents are recorded using a 16-bit data acquisition system. For a six-pole BLDC motor, the rotor fault frequencies can be calculated from (1) to be 1/3rd, 2/3rd, 4/3rd, and 5/3rd times the fundamental frequency. Non-stationary operation is implemented using sinusoidal and triangular speed references (ω^* in Fig. 7). A typical sinusoidal speed reference used in the experiments is given by

$$\omega^*(t) = 2.5\sin(2\pi q t), \tag{12}$$

where q is any frequency between 0 to 15 Hz. This frequency range adequately represents the non-stationarity encountered in several practical applications. The speed varies from 600 rpm to 1800 rpm.

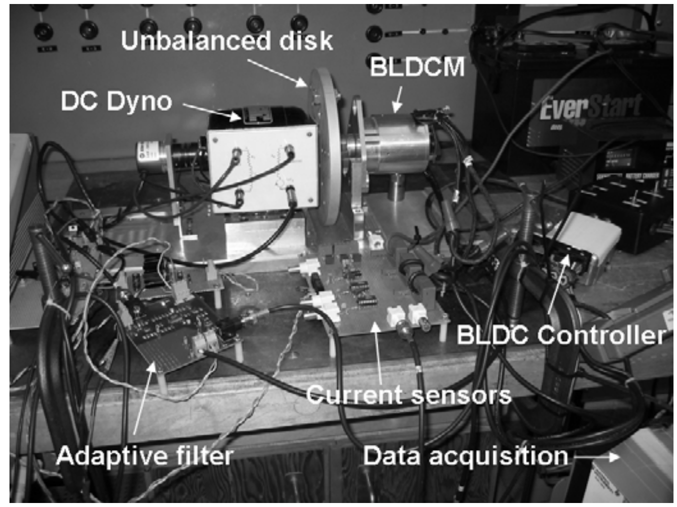

Figure 8. Experimental arrangement to implement BLDC rotor faults.

A. *Mechanically unbalanced motor*

A mechanically unbalanced rotor is implemented by mounting a slotted disk on the shaft of the motor (Fig. 8). A bolt is positioned into one of the slots on the disk thereby causing an unbalance on the rotor. Such an unbalanced disk causes slight dynamic eccentricity besides vibration and pulsating torques. The filtered real-valued stator current recorded by the data acquisition system at a sampling rate of 2 kHz is first transformed into an analytic signal using (7) and (8). The SPWVDs of the analytic filtered stator current of both a mechanically unbalanced and a mechanically balanced BLDC motor are calculated using (5). The respective SPWVDs are shown in the t-f plots of Figs. 9 and 10, which display fault frequencies as a function of time. The speed is varied sinusoidally at a frequency of 3 Hz ($q = 3$ in (12)) in this case. An adaptive filter with a fundamental notch attenuation of 30 dB is used. The SPWVD is computed with a Hamming window as the smoothing functions. The length of the time-smoothing Hamming window is 411 samples and the length of the frequency smoothing hamming window is 513 samples. These lengths are determined through trial and error to obtain the best possible time-frequency representation. Fig. 9 (mechanically balanced motor) clearly contains the fault frequencies that are not present in Fig. 10 (mechanically unbalanced motor).

B. *Dynamic Eccentricity*

Dynamic eccentricity is implemented by shifting the rotor from the centre of the stator by 33% of the air-gap length. The length of the air-gap being 0.75 mm, the rotor is shifted by 0.25 mm. Fig. 11 shows the t-f plot of the SPWVD of the analytic filtered stator current of the dynamically eccentric motor operating with a 5 Hz sine speed reference rate ($q = 5$ in (12)) indicating excellent frequency tracking with all cross-terms suppressed. The fundamental is completely absent due to a 60dB Butterworth filter. This filter has a higher attenuation than the filter used for diagnosing faults in a mechanically unbalanced motor. More attenuation at the fundamental frequency is needed to prevent cross-terms occurring due to the Wigner distributions, as the fault harmonics have smaller amplitudes for motors with dynamic eccentricity than when compared to motors with a mechanical unbalance.

Once the rotor fault frequencies for the dynamically eccentric motor have been extracted using the SPWVD (Fig. 11), a fault metric can be calculated from the amplitudes of the instantaneous fault frequencies using (11). Fig. 12 shows the fault metrics calculated for both a good motor and a motor with dynamic eccentricity operating with a 5 Hz sinusoidal speed reference ($q = 5$ in (12)) as before. A clear difference can be seen in the BLDC motor with a dynamic eccentricity when compared to the good BLDC motor, indicating a fault. This fault metric can be used as an indicator for automatic detection of rotor faults in BLDC motors. Fault discrimination can be obtained by setting thresholds that can indicate a potential rotor fault. While the demonstration of the fault metric in this paper has been limited the case of dynamic eccentricity, similar fault metrics can also be calculated to monitor mechanical motor unbalance (Figs. 9 and 10).

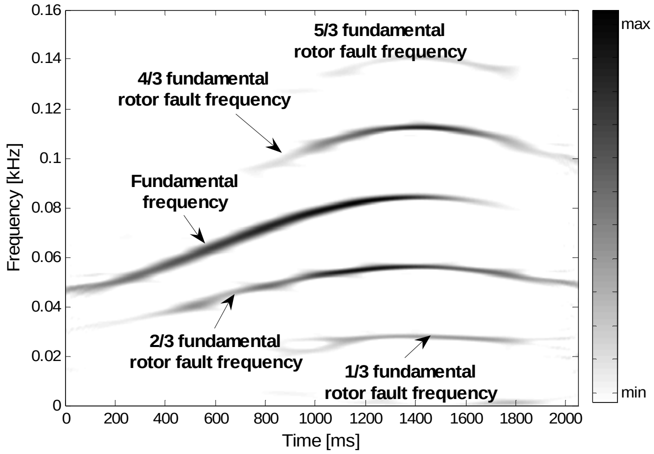

Figure 9. SPWVD of mechanically unbalanced BLDC motor (3 Hz sinusoidal speed reference).

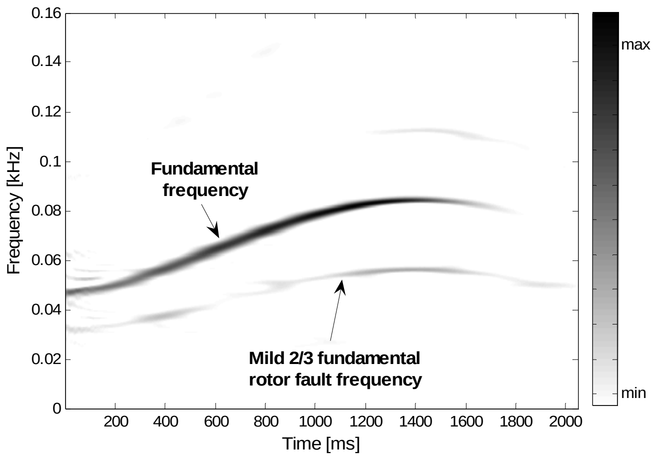

Figure 10. SPWVD of mechanically balanced BLDC motor (3 Hz sinusoidal speed reference).

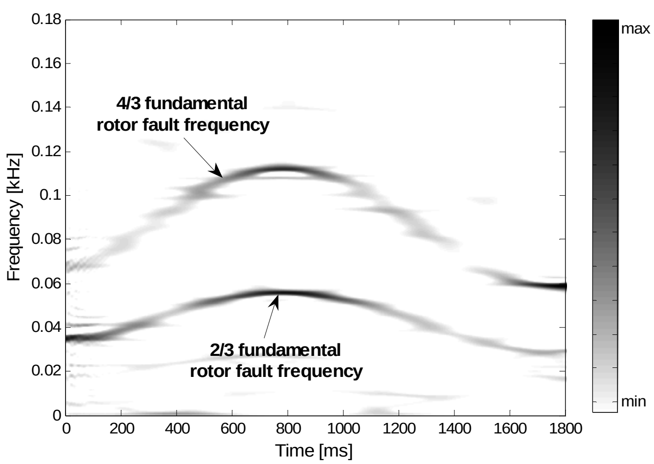

Figure 11. SPWVD of BLDC motor with dynamic eccentricity (5 Hz sinusoidal speed reference).

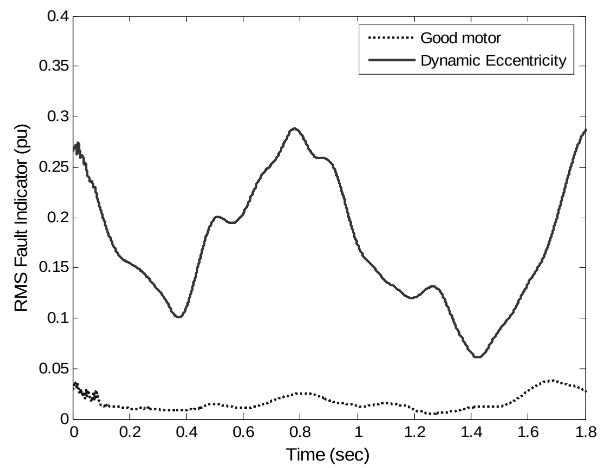

Figure 12. RMS fault indicator for fault discrimination (dynamic eccentricity).

During the experiments it is noted that the SPWVD based algorithm is able to extract frequencies from the motor stator current up to a sinusoidal speed reference of 15 Hz and a triangular speed reference of 10 Hz. This is because at such high speed reference rate increases, the current is extremely non-stationary (especially with a triangular speed reference). However such non-stationarity does not commonly occur in motor applications and any non-stationary fault detection method should take into account the severity of non-stationary behavior that may be encountered. The SPWVD based algorithm would perform very well for a vast majority of applications.

VIII. Comments on Real-Time Implementation of The WVD

Real-time implementation of WVDs is important for a practical realization of an online diagnostics scheme. The discrete PWVD (DWVD) is given by [14].

$$W_X(n,f) = 2\sum_{l=-L}^{l=L} s(n+l)\,s^*(n-l)\,w(l)\,w^*(-l)\,e^{-4\pi jl}, \quad (13)$$

where 2L+1 is the length of the signal, *w* is the chosen window function, *f* is the frequency, and *n* is the time sample. The DWVD can be optimally implemented by evaluating at time zero and shifting the signal *s(n)* so that time *n* is mapped to time origin. This is given by

$$W_X(0,f) = 2\sum_{l=-L}^{l=L} K(l)e^{-4\pi jl}, \tag{14}$$

where *K(l)* is called the DWVD kernel sequence.

$$K(l) = s(l)s^*(l)w(l)w^*(-l), \tag{15}$$

The DWVD is implemented on an ADSP-21061 digital signal processing platform to study its computational load. The Hilbert transform is implemented as a 79-tap FIR filter [14]. The kernel sequence is first computed and the discrete Fourier transform (DFT) is computed to obtain the DWVD of the sequence. Computation time for each time slice is found to be only 2.25 milli-seconds for a WVD with a rectangular window of length 1024 sample and using a 512 point FFT, thus demonstrating that the WVD can be implemented commercially in real-time.

IX. CONCLUSIONS

The use of Wigner-Ville distributions and its variants has been proposed as a viable tool to diagnose rotor faults in BLDC motors operating under continuous non-stationary conditions. The method can also be used for rotor fault detection in other types of motors such as induction motors besides BLDC motors. The effect of cross-terms and ghost can be suppressed by selective prefiltering of the current and using the Hilbert transformed version of the real-valued stator current signal. The Wigner-Ville variants, especially the SPWVD is very effective in suppressing cross-terms produced by the bi-quadratic distribution. Simulation and experimental results are provided to demonstrate the effectiveness of the Wigner-Ville distributions.

ACKNOWLEDGMENT

The authors wish to acknowledge the support of Delphi Corp., Troy, MI, and in particular the help of Dr. Tomy Sebastian (Delphi Saginaw Steering Systems), and Drs. Bruno Lequesne and Thomas W. Nehl (Delphi Research Labs),), as well as financial support from the Duke Power Company in Charlotte, North Carolina.

REFERENCES

[1] N. Bianchi, S. Bolognani, and M. Zigliotto, "Analysis of PM Synchronous Motor Drive Failures during Flux Weakening Operation," in *Proceedings of the 27th Annual IEEE Power Electronics Specialist Conference - PESC'96*, Baveno, Italy, pp.1542-1548, 1996.

[2] S. Nandi and H. A. Toliyat, "Condition monitoring and fault diagnosis of electrical machines – A review," in *Proceedings of the 34th Annual Meeting of the IEEE Industry Applications*, pp. 197-204, 1999.

[3] J. M. Cameron, W. T. Thomson, and A. B. Dow, Vibration and current monitoring for detecting airgap eccentricity in large induction motors," *IEE Proceedings*, vol. 133, pt. B, no. 3, pp.155-163, 1986.

[4] B. Yazici and G. B. Kliman, "An adaptive statistical time-frequency method for detection of broken bars and bearing faults in motors using stator current," *IEEE Trans. Industry Applications*, vol.35, no. 2, pp. 442-452, 1999.

[5] K. Kim and A. G. Parlos, "Induction motor fault diagnosis based on neuropredictors and wavelet signal processing," *IEEE/ASME Trans. Mechatronics*, vol. 7, no. 2, pp. 201-219, 2002.

[6] L. Eren and M. J. Devaney, "Motor bearing damage detection via wavelet analysis of the starting current transient," in *Proceedings of the 18th IEEE Instrumentation and Measurement Technology Conference (IMTC 2001)*, pp. 1797-1800, 2001.

[7] S. Rajagopalan, W. le Roux, R.G. Harley and T.G. Habetler, "Diagnosis of potential rotor faults in brushless DC machines," in *Proceedings of the Second International Conference on Power Electronics, Machines and Drives (PEMD 2004)*, Scotland, pp. 668-673, 2004.

[8] S. Nandi and H. A. Toliyat, "Condition monitoring and fault diagnosis of electrical machines – A review," in *Proceedings of the 34th Annual Meeting of the IEEE Industry Applications*, pp. 197-204, 1999.

[9] L. Cohen, "Time-frequency distributions – A review," *Proc. IEEE*, vol. 77, no. 7, pp. 941-981, 1989.

[10] T. A. C. M. Claasen and W. F. G. Mecklenbrauker, "The Wigner distribution – a tool for timr-frequency analysis. Part 1: continuous time signals," *Philips Journal of Research **35***, pp. 217-250, 1980.

[11] T. A. C. M. Claasen and W. F. G. Mecklenbrauker, "The Wigner distribution – a tool for timr-frequency analysis. Part 2: discrete time signals," *Philips Journal of Research **35***, pp. 276-300, 1980.

[12] B. Boashash, Time-Frequency Signal Analysis – Methods and Applications, Melbourne, Australia: Longman Cheshire, 1992.

[13] F. Auger, P. Flandrin, P. Goncalvès, and O. Lemoine, *Time-frequency toolbox for use with MATLAB*, CNRS France/Rice University, 1996.

[14] B. Boashash and P. J. Black, "An efficient real-time implementation of the Wigner-Ville distribution," *IEEE Trans. on Acoustics, Speech, and Signal Processing*, vol. 35, no. 11, 1978, pp. 1611-1618.

Paper Information

This paper was presented at the **5th IEEE Symposium on Diagnostics for Electric Machines, Power Electronics, and Drives (SDEMPED 2005),** Vienna, September 7-9, 2005 in Session – Partial Discharge and Synchronous Machine Diagnostics.

Author information:

Satish Rajagopalan
W312 Van Leer Electrical Engineering Building
Georgia Institute of Technology
777 Atlantic Dr. NW
Atlanta, Georgia 30332, USA
Phone: 404 894 5563
rsatish@ece.gatech.edu

José A. Restrepo
Universidad Simón Bolívar
Caracas 1080A, VENEZUELA
restrepo@usb.ve

José M. Aller
Universidad Simón Bolívar
Caracas 1080A, VENEZUELA
jaller@usb.ve

Thomas G. Habetler (Corresponding Author)
E171 Van Leer Electrical Engineering Building
Georgia Institute of Technology
777 Atlantic Dr. NW
Atlanta, Georgia 30332, USA
Phone: 404 894 9829
Fax: 404 894 4641
thabetler@ece.gatech.edu

Ronald G. Harley
E171 Van Leer Electrical Engineering Building
Georgia Institute of Technology
777 Atlantic Dr. NW
Atlanta, Georgia 30332, USA
Phone: 404 894 1876
Fax: 404 894 4641
ron.harley@ece.gatech.edu